MOLECULAR PHYSICS, 1991, VOL. 74, NO. 1, 161–176

A bridge between Fischer and Boublik thermodynamic perturbation theories: calculating thermodynamic properties of pure substances

By P. PADILLA, S. LAGO and C. VEGA
Departamento Quimica Fisica, Fac. Ciencias Quimicas, Universidad Complutense, 28040 Madrid, Spain

(*Received 2 May 1990; accepted 5 February 1991*)

A bridge theory between Boublik and Fischer thermodynamic perturbation theories is proposed. The fluid models studied here are composed of linear particles interacting through a pair potential depending on the shortest distance between cores, modelled as rods. This perturbation scheme has been used to predict the thermodynamic properties of two pure fluid models composed by particles of quite different anisotropy. In general, the quality of the theoretical predictions for thermodynamic properties are better for the less anisotropic model. The larger the anisotropy and the packing fraction, the greater are the discrepancies between theory and simulation. The results shown here seem, however, to be less dependent on the elongation than those of the previous perturbation theories, and the theory works better when the temperature increases. Results for spherical harmonic components of the reference system pair correlation function are compared with available Monte Carlo (MC) simulation data. The discrepancies between theory and simulation increase with the packing fraction and the anisotropy of the model.

1. Introduction

In statistical mechanical studies of molecular fluids two aspects have to be considered: model potentials and the theoretical framework to obtain the properties of the model. The former aspect: the assumption of a model potential to represent the interactions between particles in a real fluid is a matter of quantum mechanics. From a purely statistical mechanical point of view, however, the model potential has to be an intermediate situation between an accurate representation of actual interactions and a tractable analytic potential function. Several relatively simple model potentials have been proposed to account for the interactions between non-polar molecules. The interaction site model (ISM) [1–3] potential has been the most profusely studied though other model potentials, as Kihara [4] or Gaussian overlap [5] models have the advantage over ISM that the potential functions retain their simplicity even when more complex molecules are considered. In spite of this advantage of Kihara models, only a relatively small amount of theoretical work [6–8] and a few simulations [8, 9] for this model potential have been carried out. The main reason for this seems to be the difficulties in the evaluation of the shortest distance between cores. This trouble has been already solved by one of us [10] for the particular case of representing molecular cores as rods. We are interested now in using this model potential to represent linear molecules like N_2, Cl_2, CO_2 and even more complex molecules, which can be modelled as simply linear, like C_2H_4 and C_2H_6.

In this paper we present a 'bridge' theory between the Boublik and Fischer thermodynamic perturbation theories for the purpose of obtaining the thermodynamic

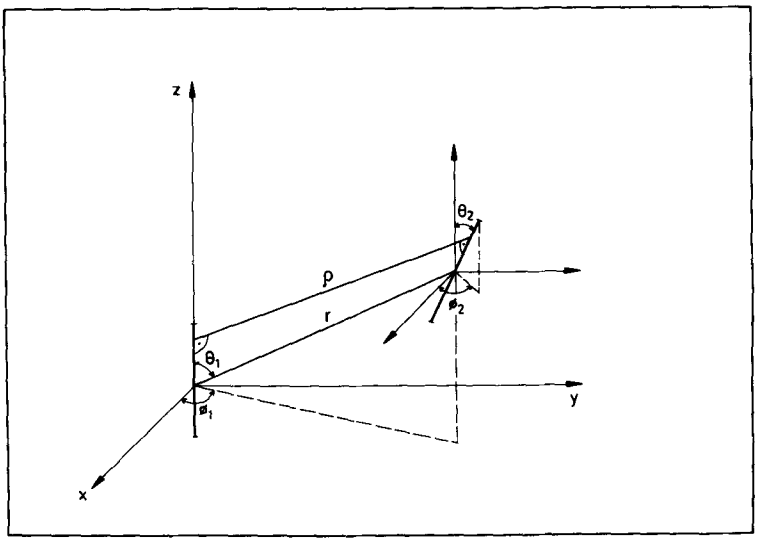

Figure 1. Illustration of the dependence of the shortest distances between cores on the orientation of the particles.

properties of Kihara models with molecular cores modelled as rods. Boublik has already proposed several perturbation treatments [6–8] for the study of Kihara models, but in all of them a semiempirical approximation for the structure of the reference system must be used. The Percus–Yevick (PY) equation has been recently solved [11] for hard spherocylinders and for a purely repulsive Kihara model [12]. The numerical procedure in both cases is too complex to serve as a practical means of evaluating the structure of the reference system in a perturbation scheme, and so we used Fischer [1] approximation to evaluate g^0.

Thus, the scheme of the paper is as follows: section 2 is devoted to describing the model studied here and the theory used to obtain the thermodynamic properties of the model. Numerical results for Helmholtz free energy, internal energy and compressibility factor are shown in section 3, where they are compared first with simulation results and then with experimental results for a nitrogen model and for a model with $L^* = 1$. A brief discussion of the thermodynamic results is also presented in section 3. Reference system structure results are compared with available MC simulation data in section 4. Some relevant conclusions are presented in section 5.

2. Theory

2.1. *Model*

We consider a system of linear or quasilinear molecules in the canonical ensemble. These particles can be modelled through an additive pairwise intermolecular interaction, where the pair interaction is a Kihara [4] potential with a rod as a core. The potential between two molecules i and j at centre-of-mass–centre-of-mass distance $\boldsymbol{r}_{ij}$ and with orientations ω_i and ω_j depends on the shortest distance, $\rho(r_{ij}, \omega_i, \omega_j)$, between their molecular cores (see figure 1). For the sake of clarity, hereafter we will denote $\rho(r_{ij}, \omega_i, \omega_j)$ simply as ρ. The analytical potential function is

$$u(\rho) = 4\varepsilon[(\sigma/\rho)^{12} - (\sigma/\rho)^6], \tag{1}$$

where σ and ε are the characteristic parameters of the potential with dimensions of length and energy, respectively. The anisotropy of the molecules is characterized by the ratio between the length of the rod, L, and the parameter σ of the potential. This ratio is denoted by L^*. We try to use this model to represent actual linear molecules like N_2, Cl_2 or acetylene as well as slightly more complicated molecules such as ethylene or ethane. Hereafter, we use the following reduced magnitudes:

$$T^* = kT/\varepsilon, \tag{2}$$

$$\eta = \pi\sigma^3 n/6(1 + 3L^*/2), \tag{3}$$

where n is the numerical density and η is usually called the packing fraction.

2.2. *Perturbation expansion for linear molecules*

The central idea of perturbation theories is to expand the thermodynamic properties of the system of interest in terms of the properties of a reference system whose properties are better known. In the case of polyatomic fluids, several alternatives are possible, but we refer here only to those more closely related to our work. In the Mo and Gubbins [2] division, the full intermolecular potential, $u(\boldsymbol{r}_{12}, \omega_1, \omega_2)$, is thus divided as:

$$u(\boldsymbol{r}_{12}, \omega_1, \omega_2) = u^0(\boldsymbol{r}_{12}, \omega_1, \omega_2) + u^1(\boldsymbol{r}_{12}, \omega_1, \omega_2), \tag{4}$$

$$u^0(\boldsymbol{r}_{12}, \omega_1, \omega_2) = u(\boldsymbol{r}_{12}, \omega_1, \omega_2) + \varepsilon(\omega_1, \omega_2), \qquad r \leqslant r_m(\omega_1, \omega_2), \tag{5a}$$

$$= 0, \qquad r > r_m(\omega_1, \omega_2), \tag{5b}$$

$$u^1(\boldsymbol{r}_{12}, \omega_1, \omega_2) = -\varepsilon(\omega_1, \omega_2), \qquad r \leqslant r_m(\omega_1, \omega_2), \tag{6a}$$

$$= u(\boldsymbol{r}_{12}, \omega_1, \omega_2), \qquad r > r_m(\omega_1, \omega_2), \tag{6b}$$

where, the superscripts 0 and 1 refer respectively to the reference and to the perturbation potential. $\varepsilon(\omega_1, \omega_2)$ is the potential depth and $r_m(\omega_1, \omega_2)$ is the centre–centre distance, both evaluated at the minimum of the pair potential (for fixed ω_1 and ω_2). According to this division [1], the perturbation expansion for the excess Helmholtz free energy up to the first-order term is

$$A^{exc} = A^0 + \frac{Nn}{2} \int d\boldsymbol{r}_{12} \langle u^1(r_{12}, \omega_1, \omega_2) g^0(r_{12}, \omega_1, \omega_2) \rangle_{\omega_1, \omega_2}, \tag{7}$$

where the brackets denote unweighted averaging over ω_1 and ω_2, and N is the number of particles.

For Kihara potential models, the Mo and Gubbins division can be easily written as

$$u^0(\rho) = u(\rho) + \varepsilon, \qquad \rho \leqslant 2^{1/6}\sigma, \tag{8a}$$

$$u^0(\rho) = 0, \qquad \rho > 2^{1/6}\sigma, \tag{8b}$$

$$u^1(\rho) = -\varepsilon, \qquad \rho \leqslant 2^{1/6}\sigma, \tag{9a}$$

$$u^1(\rho) = u(\rho), \qquad \rho > 2^{1/6}\sigma. \tag{9b}$$

Now, in (7) A^0 and $g^0(\boldsymbol{r}_{12}, \omega_1, \omega_2)$ correspond to a system of particles interacting with the potential function defined in (8). The properties of such a system have already been obtained by solving [12] the corresponding Percus–Yevick (PY) equation, but the numerical procedure for resolution of that equation is a very expensive computation. Several approximations are needed in order to obtain A^0 and $g^0(\boldsymbol{r}_{12}, \omega_1, \omega_2)$.

A^0 can be approximated as the Helmholtz free energy of a system of hard spherocylinders (HSC), A^{HSC}, using a blip expansion [1]. The thickness, σ^{HSC}, of the corresponding hard spherocylinder is chosen to eliminate the first perturbation term. When it is used along with the general assumption that the length of the axis of the hard spherocylinder is equal to the length, L, of the molecular core, σ^{HSC} is the solution of the equation

$$\int_0^\infty d\rho\, S_{c+\rho+c} y_{HSC}^{ave}(\rho) \left[\exp\left(\frac{-u^0(\rho)}{kT} \right) - \exp\left(\frac{-u^{HSC}(\rho)}{kT} \right) \right] = 0, \tag{10}$$

where $S_{c+\rho+c}$ is the mean surface formed by the origin of a core when it moves around another core at constant distance ρ. $y_{HSC}^{ave}(\rho)$ is the average background correlation function of the hard spherocylinder system defined in terms of the average correlation function $g^{ave}(\rho)$ as:

$$y^{ave}(\rho) = g^{ave}(\rho) \exp(u(\rho)/kT). \tag{11}$$

$S_{c+\rho+c}$ can be expressed in terms of the geometrical functionals of the molecular cores (rods):

$$S_{c+\rho+c} = 2S_c + 8\pi R_c^2 + 16\pi R_c \rho + 4\pi\rho^2, \tag{12}$$

where R_c denotes the mean curvature integral. For the model potential defined in (8) $S_c = 0$ and $R_c = L/4$, and (10) can then be written as:

$$\begin{aligned} &\frac{\pi L^2}{2} \int d\rho\, y_{HSC}^{ave}(\rho) \left[\exp\left(\frac{-u^0(\rho)}{kT} \right) - \exp\left(\frac{-u^{HSC}(\rho)}{kT} \right) \right] \\ &+ 4\pi L \int d\rho\, y_{HSC}^{ave}(\rho) \left[\exp\left(\frac{-u^0(\rho)}{kT} \right) - \exp\left(\frac{-u^{HSC}(\rho)}{kT} \right) \right] \rho \\ &+ 4\pi \int d\rho\, \rho^2 y_{HSC}^{ave}(\rho) \left[\exp\left(\frac{-u^0(\rho)}{kT} \right) - \exp\left(\frac{-u^{HSC}(\rho)}{kT} \right) \right] = 0 \end{aligned} \tag{13}$$

However, in order to solve (13) it is necessary to know $y_{HSC}^{ave}(\rho)$, and unfortunately we have not yet found a practicable way to evaluate such a function. This trouble is overcome when a Barker–Henderson (BH) perturbation expansion of A^0 about A^{HSC} is used. From the Boublik [6] extension of the BH theory to convex bodies, σ^{HSC} can be obtained as

$$\sigma^{HSC} = \int_0^{2^{1/6}\sigma} d\rho \left[\exp\left(\frac{-u^0(\rho)}{kT} \right) - 1 \right]. \tag{14}$$

The integration in (14) is done numerically by the Simpson rule. Once the size of the hard spherocylinder is known, the hard convex body equation of state of Boublik and Nezbeda [13] is used to obtain A^{HSC}.

The structure of the reference system can be obtained by applying the approximations introduced by Fischer [1] in his thermodynamic perturbation theory. An angle-averaged spherical potential is defined by

$$\exp\left(\frac{-\phi(r)}{kT} \right) = \left\langle \exp\left(\frac{-u^0(\mathbf{r}, \omega_1, \omega_2)}{kT} \right) \right\rangle_{\omega_1, \omega_2}. \tag{15}$$

The orientationally dependent pair correlation function is approximated by a zero-order perturbation expansion of the background correlation function, $y^0(\mathbf{r}_{12}, \omega_1, \omega_2)$,

of the reference system around $\phi(r_{12})$, namely:

$$y(\boldsymbol{r}_{12}, \omega_1, \omega_2) = \hat{y}(r_{12}), \tag{16}$$

where $\hat{y}(r_{12})$ is the background correlation function corresponding to the system interacting through $\phi(r_{12})$.

Finally, the expression for $g^0(\boldsymbol{r}_{12}, \omega_1, \omega_2)$ is:

$$g^0(\boldsymbol{r}_{12}, \omega_1, \omega_2) = \hat{y}(r_{12}) \exp(-u^0(\boldsymbol{r}_{12}, \omega_1, \omega_2)/kT). \tag{17}$$

Substitution of A^0 and $g^0(\boldsymbol{r}_{12}, \omega_1, \omega_2)$ in (7) gives

$$A^{\text{exc}} = A^{\text{HSC}} + \frac{Nn}{2} \int \mathrm{d}\boldsymbol{r}_{12} \hat{y}(r_{12}) \langle u^1(\boldsymbol{r}_{12}, \omega_1, \omega_2) \exp(-u^0(\boldsymbol{r}_{12}, \omega_1, \omega_2)/kT) \rangle_{\omega_1, \omega_2}. \tag{18}$$

When the orientational average of the actual pair correlation function of the Kihara system (PCF) is simply approached by the PCF of the reference system the internal energy, E, is obtained as

$$E^{\text{exc}} = \frac{Nn}{2} \int \mathrm{d}\boldsymbol{r}_{12} \langle u(\boldsymbol{r}_{12}, \omega_1, \omega_2) g^0(\boldsymbol{r}_{12}, \omega_1, \omega_2) \rangle_{\omega_1, \omega_2}, \tag{19}$$

or

$$E^{\text{exc}} = \frac{Nn}{2} \int \mathrm{d}\boldsymbol{r}_{12} \hat{y}(r_{12}) \langle u(\boldsymbol{r}_{12}, \omega_1, \omega_2) \exp(-u^0(\boldsymbol{r}_{12}, \omega_1, \omega_2)/kT) \rangle_{\omega_1, \omega_2}. \tag{20}$$

The superscript exc for the Helmholtz and internal energies in the above equations denotes differences with respect to the ideal value. $\hat{y}(r_{12})$ is obtained by numerically [1] solving the corresponding PY equation for $\phi(r_{12})$ in the Baxter formulation [14]. The integrals corresponding to the average values have been performed by Conroy's method [15]. From a practical point of view, the time of computation of each isotherm is limited by the time of computation of the solution of the PY equation. On the other hand, it should be remarked that the calculation of the average for the energy expression in (20) is not dependent on the accuracy with which the PY equation is solved. This method is certainly less ambiguous than the numerical derivation of the Helmholtz free energy using thermodynamic relations, because in the case of numerical derivation, results strongly depend on the algorithm and on the number of points where A was obtained. The influence of the potential range on the computation of averages has been discussed elsewhere [16].

3. Results for thermodynamic properties

The perturbation theory presented here can be applied to a variety of molecular fluids. We show here the results obtained for the thermodynamic properties of fluid nitrogen, which has a small elongation ($L^* = 0{\cdot}29$), and for a model fluid with $L^* = 1{\cdot}0$, which is larger than that of most important molecular fluids. These two fluids have been chosen because to our knowledge they are the only ones for which simulation results exist for the potential function in (1).

3.1. *Results for nitrogen*

The calculations for nitrogen have been made for states in the range $70\,\text{K} \leqslant T \leqslant 160\,\text{K}$ and $3 \times 10^{-3}\,\text{Å}^{-3} \leqslant n \leqslant 2 \times 10^{-2}\,\text{Å}^{-3}$ corresponding to fluid phases.

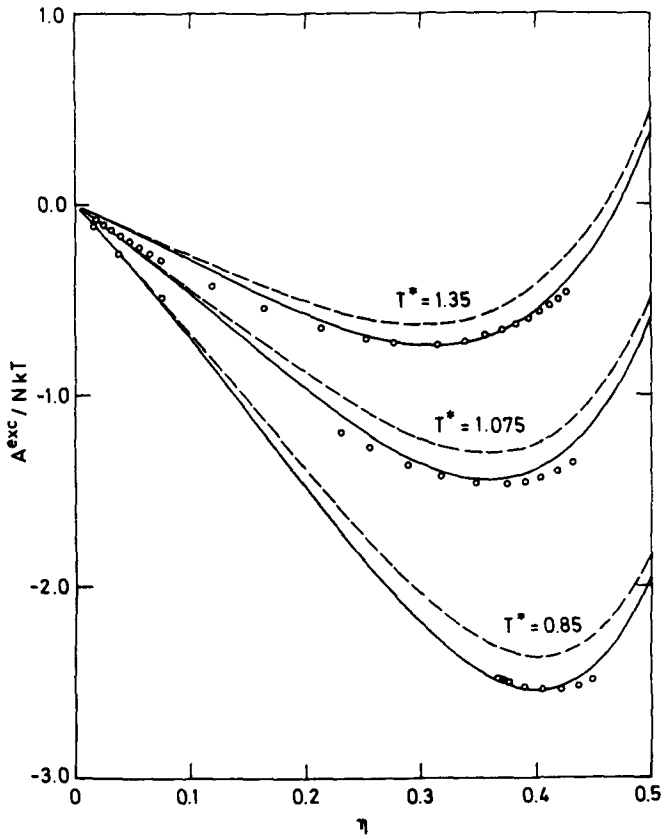

Figure 2. Free Helmholtz energy data at reduced temperatures 0·85, 1·075 and 1·35 (—— this work, – – – Boublik predictions [6], ···· experimental data).

Two sets of parameters from the literature [4, 8] have been used to represent the pair interaction of fluid nitrogen. Kihara [4] parameters obtained from experimental data for the second virial coefficient are $\sigma = 3{\cdot}207$ Å, $L^* = 0{\cdot}29$ and $\varepsilon/K = 117$ K. Boublik [8] parameters obtained by fitting saturation properties of the liquid N_2, are $\sigma = 3{\cdot}216$ Å, $L^* = 0{\cdot}289$ and $\varepsilon/k = 113{\cdot}94$ K.

In figure 2 we compare our results for the excess Helmholtz free energy and the predictions obtained by Boublik [6], for the nitrogen model with Kihara [4] parameters. Experimental data from reference [17] are also represented in figure 2. Our theoretical results show better agreement with experimental data than those of Boublik. Since both theories use the same approximation to evaluate A^0, the differences between both theoretical predictions should come from the evaluation of A^1, i.e., from the evaluation of the reference system structure. Boublik describes the structure in terms of the average correlation function, $g^{ave}(\rho)$, which is obtained as an empirical function by fitting to simulation data, and this fact limits the generalization of the theory. We, however, described the structure in terms of the pair correlation function $g(r_{12}, \omega_1, \omega_2)$ with approximation (17), which can be applied, in principle, to any elongation of the molecular core, and, therefore, any correction to this approximation can be systematically designed.

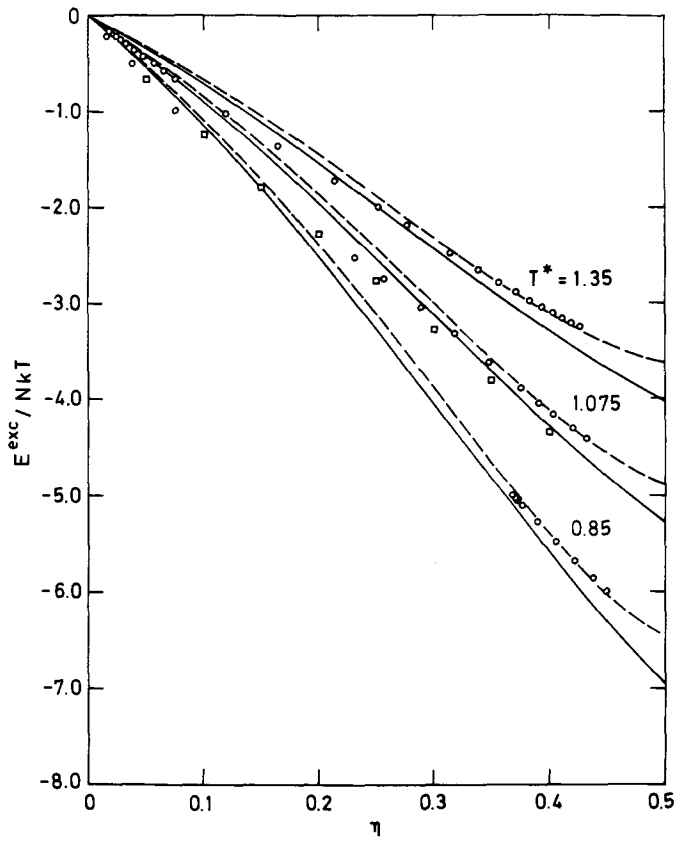

Figure 3. Internal energy data at same reduced temperatures as figure 1 (——, this work, – – – Boublik predictions [6], ○ experimental data [17] and □ simulation results [9]).

The best agreement between our theoretical results and the experimental data appears in the intermediate range of packing fractions. The source of errors in the low density range seems to be obvious: the convergence of the perturbation expansion in this range is slow. It should, therefore, be expected that more than two terms are needed for an accurate description of the thermodynamic properties of the fluid. On the other hand, in the high-density range, a first-order perturbation expansion should be enough to predict thermodynamic properties, so in this range the main source of errors seems to be the evaluation of the reference system properties. As is shown in [9] the approximation used to obtain A^0 overestimates its value in the high density range. An alternative equation of state [18] was used in order to evaluate A^0, but we did not find any significant improvement. Furthermore, as will be discussed below, approximation (17) for $g^0(\boldsymbol{r}_{12}, \omega_1, \omega_2)$ worsens as the density increases.

Figure 3 displays the Boublik results and our own predictions for excess internal energy for the Kihara model of nitrogen, along with experimental values and simulation data from [9]. A good agreement between theoretical and experimental data is found. Our theoretical predictions are consistently more negative than those of Boublik. It should be noted that Boublik obtained the internal energy from the derivative of A^{exc}/NkT while we obtained it from (20). At high packing fractions, Boublik's results show better agreement than ours with experimental data. Opposing

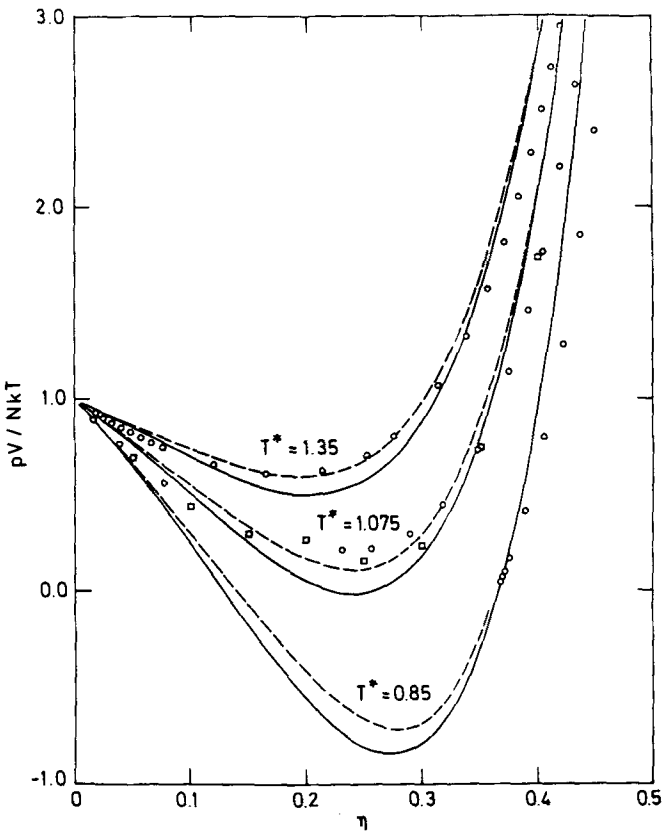

Figure 4. Compressibility factor data. Symbols and temperatures as in figure 2.

behaviour is found when both theoretical predictions are compared with simulation data [9].

The compressibility factor is obtained from the derivative of Helmholtz free energy as

$$\begin{aligned} Z &= Z^0 + n(\partial A^1/\partial n)_T, \\ &= Z^{HSC} + n(\partial A^1/\partial n)_T, \end{aligned} \tag{21}$$

where Z^{HSC} is the compressibility factor of the corresponding hard spherocylinder system obtained by an EOS of hard convex bodies, and A^1 is the first perturbation term.

The results for the Kihara model of nitrogen are shown in figure 4. In a comparison with experimental data, the agreement increases as the temperature does for both theoretical predictions and moreover, the results overestimate the compressibility factor at high packing fractions. In general, our theoretical predictions are better than those of Boublik in the low and high density ranges. At intermediate densities, Boublik's results reproduce the experimental data better than ours. When a comparison with available MC data from [9] is considered, we found that our results reproduce the simulation data quite well, except in the range of intermediate packing fractions. It must be said that the simulation data correspond to $T^* = 1{\cdot}075$, which is very close to experimental critical temperature of nitrogen and furthermore, the

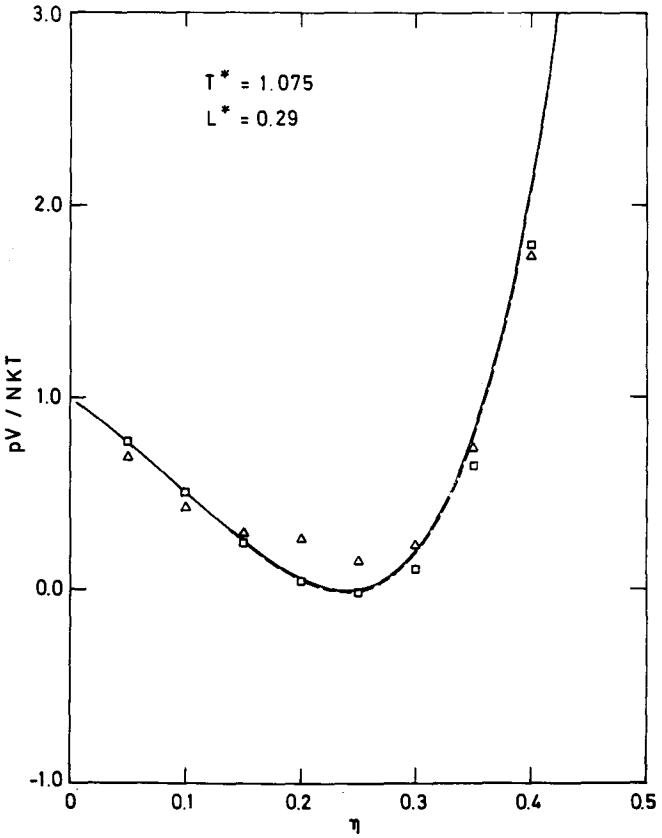

Figure 5. Compressibility factor data for $L^* = 0{\cdot}29$ at $T^* = 1{\cdot}075$ (——) theoretical predictions using EOS from [6] (– – –)id. using EOS from reference [18]; (□) semitheoretical predictions (see text); (△) simulation data [9].

packing fraction corresponding to the critical density is about 0·17. We, therefore, felt that the simulation data close to this packing fraction should be considered with caution.

In order to analyse the sources of errors of the theory, theoretical results for the compressibility factor of the Kihara model of nitrogen at $T^* = 1{\cdot}075$, along with simulation data, are displayed in figure 5. The solid line corresponds to results obtained from (21) by calculating Z^{HSC} with an EOS proposed in reference [6]. The dashed line corresponds to results obtained using an EOS proposed in [18]. It can be seen from figure 5, that for this model with a small value of L^*, there is not any clear improvement when different EOS for hard convex bodies are used, as is noted below. The squares in figure 5 correspond to semitheoretical results obtained when the 'exact' value of Z^0 from the simulation data of [9] is used in (21). When these results are compared with the purely theoretical predictions, it is found that the differences between both sets of results are not significant up to $\eta = 0{\cdot}25$, but at higher densities a significant error is introduced by our approximation for Z^0, and hence for A^0. Then, when those semitheoretical results are compared with the simulation data for the full system (triangles) [9], we found that the agreement between both results improves as density increases. The remaining discrepancies at $\eta = 0{\cdot}4$ are very small and could

Table 2. Compressibility factor of a Kihara model with $L^* = 1{\cdot}0$.

T^*	η	Z^a	Z^b	Z^c
0·85	0·1414	0·24	0·31	0·26
	2·2245	0·10	0·20	−0·02
	0·3351	0·28	1·44	0·29
1·00	0·1414	0·47	0·55	0·51
	0·2245	0·41	0·60	0·40
	0·3351	1·02	1·99	0·98
1·15	0·1414	0·62	0·73	0·68
	0·2245	0·64	0·89	0·70
	0·3351	1·62	2·38	1·48
1·35	0·1414	0·83	0·90	0·85
	0·2245	1·02	1·17	1·00
	0·3351	1·97	2·75	1·95

[a] Simulation data from [8]
[b] This work.
[c] Theoretical predictions from [8].

derive from approximation [17]. For this model, therefore, the main source of errors in the liquid densities range, where a first-order perturbation theory should reproduce the thermodynamic properties of the model, seems to be the approximation for A^0.

In general, we can say that our theory gives a better agreement with simulations than Boublik's theory. To further clarify this point, we checked how sensitive the results of our theory are to the choice of a set of parameters [4, 8] and we found no meaningful differences between the two models, since the results are expressed in terms of reduced magnitudes and the value of L^* is about the same for both models. When theoretical results are compared with each corresponding set of experimental data, it is found, however, that theoretical predictions with Kihara parameters [4] show better agreement with experimental data. Furthermore, A^{exc}/NkT appears to be more sensitive to the choice of parameters of the potential than E^{exc}/NkT and pV/NkT. The very general conclusion that simulations are the only correct way to decide in which extension a theory is valid, is strengthened here once again. In this sense the theory presented here is a clear improvement on the Boublik results [6].

3.2. *Results for* $L^* = 1$

We have also made some calculations for $L^* = 1$ for states corresponding to the reduced temperatures $T^* = 0{\cdot}75, 0{\cdot}85, 1{\cdot}0, 1{\cdot}15, 1{\cdot}35$.

In tables 1 and 2 theoretical predictions of the compressibility factor and the internal energy are respectively shown along with the theoretical results and simulation data from Boublik [8]. As expected, the agreement between theory and simulation data is worse than it was for the nitrogen model.

Again, for analysis of the sources of error of the theory, figure 6 shows theoretical results along with simulation data [8] for the compressibility factor of the model with $L^* = 1{\cdot}0$ at $T^* = 1{\cdot}0$. Now, the differences between the theoretical results obtained with (21) and Z^{HSC} obtained from different hard convex bodies EOSs, are larger than those for $L^* = 0{\cdot}29$, and the improvement introduced by using the EOS from [18] is again small in comparison with the differences with the simulation data. When the 'exact' value of Z^0 obtained by MC is introduced in (21), the results improve slightly. The remaining differences are still large and they sould come from approximation

Table 2. Internal energy of a Kihara model with $L^* = 1{\cdot}0$.

T^*	η	E/NkT[a]	E/NkT[b]	E/NkT[c]
0·85	0·1414	−2·08	−1·44	−1·68
	0·2245	−3·04	−2·45	−2·67
	0·3351	−4·33	−3·89	−4·13
1·00	0·1414	−1·60	−1·21	−1·38
	0·2245	−2·42	−2·06	−2·21
	0·3351	−3·60	−3·27	−3·43
1·15	0·1414	−1·30	−1·05	−1·17
	0·2245	−2·04	−1·78	−1·88
	0·3351	−3·05	−2·81	−2·91
0·85	0·1414	−1·05	−0·89	−0·96
	0·2245	−1·66	−1·50	−1·56
	0·3351	−2·52	−2·35	−2·41

[a] Simulation data from [8].
[b] This work.
[c] Theoretical predictions from [8].

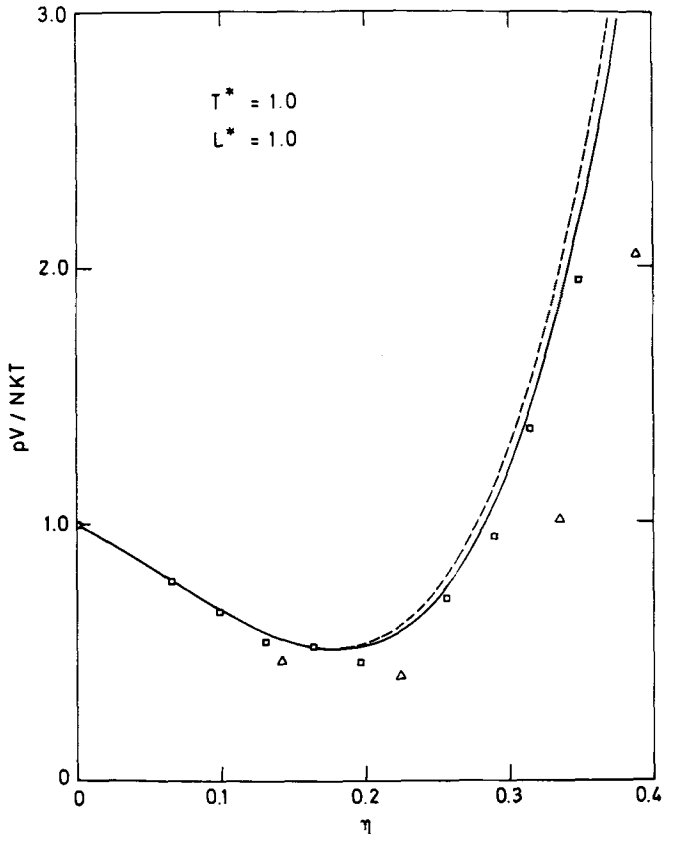

Figure 6. Compressibility data for $L^* = 1{\cdot}0$ at $T^* = 1{\cdot}0$. (– – –) theoretical predictions using EOS from reference [6]; (– – –)id. using EOS from reference [18]; (□) semitheoretical predictions (see text); (△) simulation data [8].

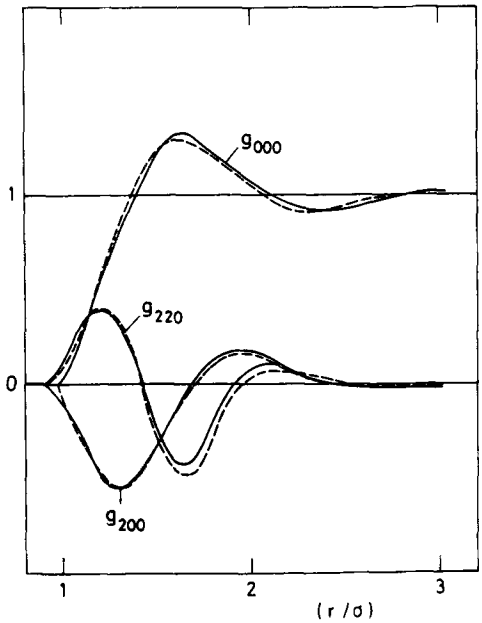

Figure 7. First coefficients of the spherical harmonic expansion of $g(r_{12}, \omega_1, \omega_2)$. (—— reference system (5) for $L^* = 1{\cdot}0$ at $T^* = 1{\cdot}0$, – – – hard spherocylinders with $L^* = 1{\cdot}0$).

(17). For $L^* = 1{\cdot}0$ the main source of errors seems, therefore, to be the approximation for the reference system structure.

Both the theoretical predictions overrate the internal energy, but ours appears systematically less negative than Boublik's results. The differences between both theoretical results and simulation data decrease when temperature increases. The same trend was found in the Kihara nitrogen model when theoretical results were compared with experimental data [17]. The reason for such an improvement in our theoretical predictions for internal energy as temperature increases, could lie in the loss of structure of the full system when temperature rises, and consequently (20) should become a better approximation for E^{exc}/NkT.

In table 1 we found that there is no systematic variation of the discrepancies between our theoretical results and simulation data, with packing fraction. Again, however, there is an improvement in our theoretical predictions as the temperature increases. The origin of such an improvement could be due to the decrease in weight of the perturbation term in (18), since, as can be seen from figure 7, there is no significant dependence of the reference system structure on temperature.

4. Results for reference system structure

In order to test the quality of approximation (17) we obtained the spherical harmonic components for $l_1 l_2 m = 000, 200, 220$ and 221 of $g^0(r_{12}, \omega_1, \omega_2)$, and these were compared with MC data [9, 19] for the two models studied here.

Results for $g^0_{000}(r)$ for $L^* = 0{\cdot}29$ at $T^* = 1{\cdot}075$ and at packing fractions 0·2, 0·3, and 0·4 along with MC simulation data, are shown in figure 8. The positions and peak heights are accurately described even at the highest packing fraction. Approximation (17) seems, therefore, to be enough to describe the correlations between the centres of the particles. The results for $g^0_{200}(r)$ and $g^0_{220}(r)$ are not so satisfactory, as is shown

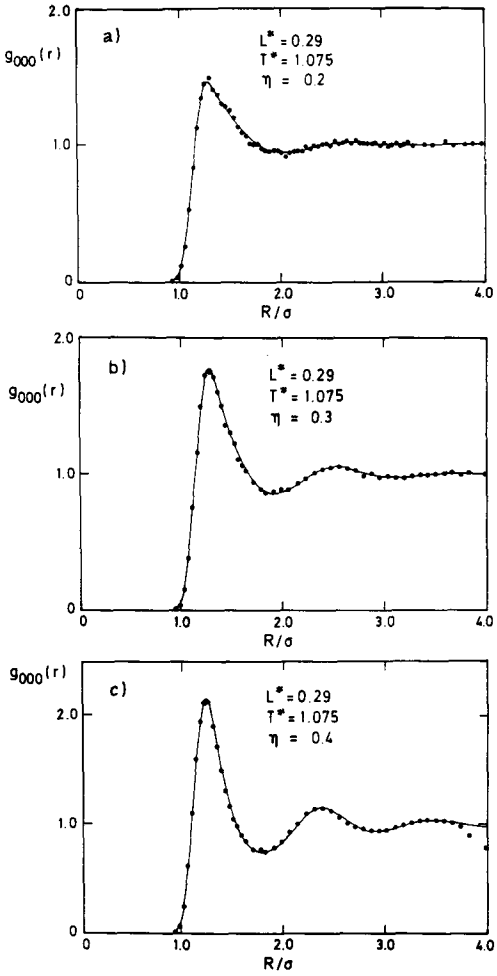

Figure 8. $g^0_{000}(r)$ for $L^* = 0.29$ at $T^* = 1{\cdot}075$ at three packing fractions. (a) $\eta = 0{\cdot}2$; (b) $\eta = 0{\cdot}3$; (c) $\eta = 0{\cdot}4$. (——) theory (●) simulation [19].

in figure 9; the results for $g^0_{221}(r)$ are not displayed because its value is comparatively too small. In general, the theoretical results show the correct shape. For $\eta = 0{\cdot}2$ the agreement is quantitative. As the density increases, however, the orientational correlations appear to be correctly described at smaller values of r but underpredicted at large and intermediate r values; in general they are short ranged.

Figure 10 shows the results for $L^* = 1{\cdot}0$ at $T^* = 1{\cdot}0$ for the four spherical harmonic components written above, along with simulation data. For this model, the correlations between the centres of the particles are not so well described as they were for the model with $L^* = 0{\cdot}29$. However, except in the case of $\eta = 0{\cdot}4$, there is a quantitative agreement between theory and simulation. For $\eta = 0{\cdot}4$, the position of the first peak is reproduced but its height is overpredicted. The other spherical harmonic components show a quantitative agreement with simulation data in the range of small values of r up to $\eta = 0{\cdot}289$. Nevertheless, the orientational correlations at intermediate and long r value range are underpredicted even for the lowest density. For $\eta = 0{\cdot}4$ the theoretical spherical harmonic components show significant

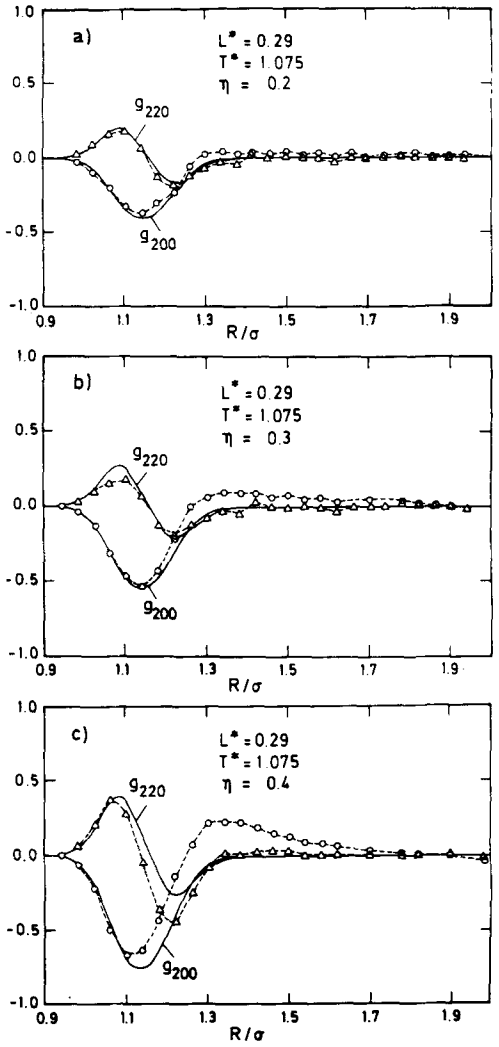

Figure 9. $g^0_{000}(r)$ and $g^0_{220}(r)$ for $L^* = 0{\cdot}29$ at $T^* = 1{\cdot}075$ at three packing fractions. (a) $\eta = 0{\cdot}2$; (b) $\eta = 0{\cdot}3$; (c) $\eta = 0{\cdot}4$. (——) theory; (○) $g^0_{200}(r)$ from simulation [19]; (△) $g^0_{220}(r)$ from simulation [19]. (Dashed lines are only for visual assistance).

discrepancies with simulation data in the whole range of r. In order to improve the theoretical results for models with large elongation like $L^* = 1{\cdot}0$, it seems to be necessary to introduce more information about the orientational correlations in the fluid in the approximation for the reference system structure.

5. Summary and conclusions

We have obtained the thermodynamic properties of two pure fluid models of linear particles with a bridge theory between the Fischer and Boublik thermodynamic perturbation theories. The most important improvement in relation to the original Fischer treatment seems to be that the results are less sensitive to elongation for the model of spherocylinders than for the dumb-bell model. On the other hand, the results shown here have a similar quality to those of Boublik, but we have not used at all an

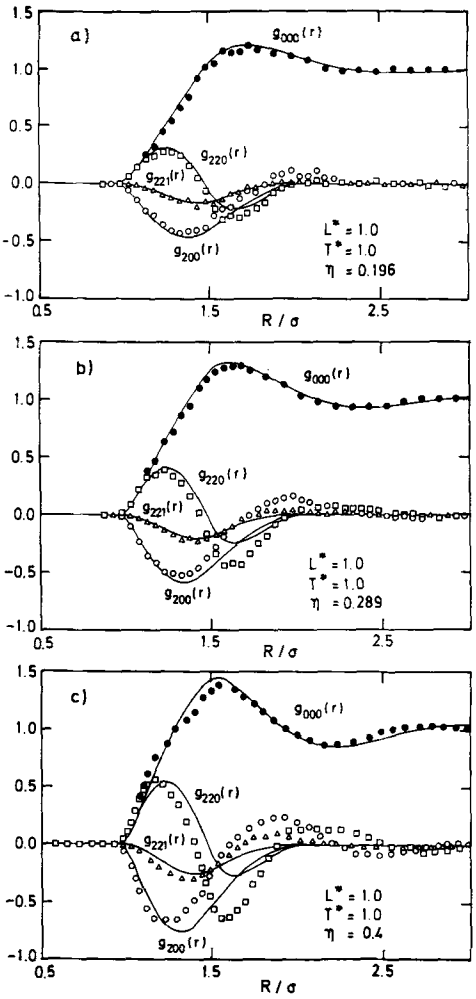

Figure 10. $g^0_{000}(r)$, $g^0_{200}(r)$, $g^0_{220}(r)$ and $g^0_{221}(r)$ for $L^* = 1{\cdot}0$ at $T^* = 1{\cdot}0$ at three packing fractions. (a) $\eta = 0{\cdot}196$; (b) $\eta = 0.289$; (c) $\eta = 0.4$. (——) theory; (●) $g^0_{000}(r)$ from simulation [19], (□) $g^0_{200}(r)$ from simulation [19]; (○) $g^0_{220}(r)$ from simulation [19]; (△) $g^0_{221}(r)$ from simulation [19].

empirical pair correlation function, and so improvements to our theory can be systematically designed.

The quality of the theoretical predictions for the properties of all the models studied improves systematically as the temperature increases. This improvement can be justified in terms of the decrease in the weight of the perturbation term in the results for free energy and compressibility factor. When the influence of the density is considered, we can reasonably state that a first-order perturbation theory is not enough to predict the thermodynamic properties in the low density range. On the other hand, in the high density range, and for $L^* = 0{\cdot}29$, the theory reproduces the simulation data quite well. The main source of errors for this model seems to be in the apprroximation to obtain A^0. However, for the model with $L^* = 1{\cdot}0$ most of the discrepancies between theoretical and simulation results stem from approximation (17).

From the comparison between theory and simulation results for the structure of the reference system, we can say that though approximation (17) in general underestimates the orientational correlations between particles, it is suitable for the treatment of models with small elongations. When models of moderate and large elongation are considered an approximation must, however, be introduced with more information on orientational correlations.

Helmholtz free energy seems to be a more sensitive property than internal energy or compressibility factor to the choice of potential parameters. When the anisotropy of the particle increases theoretical results become poorer even for internal energies.

This work was financially supported by the Project PB88-0143 of the Spanish DGICYT (Direccion General de Investigaciön Científica Y Técnica).

References

[1] FISCHER, J., 1980, *J. chem. Phys.*, **72,** 5371.
[2] MO, K. C., and GUBBINS, K. E., 1974, *Chem. Phys. Lett.*, **27,** 144.
[3] FISCHER, J., and LAGO, S., 1983, *J. Chem. Phys.*, **78,** 5750.
[4] KIHARA, T., and KOIDE, A., 1975, *Adv. Chem. Phys.*, **33,** 51.
[5] SEDIAWAN, W. B., GUPTA, S., and MCLAUGLIN, E., 1987, *Molec. Phys.*, **62,** 141.
[6] BOUBLIK, T., 1976, *Molec. Phys.*, **32,** 1737.
[7] BOUBLIK, T., 1974, *Coll. Czech. Chem. Commun.*, **39,** 2333; BOUBLIK, T., and WINKELMANN, J., 1978, *Coll. Czech. Chem. Commun.*, **43,** 2821; LAGO, S., and BOUBLIK, T., 1980, **45,** 3051.
[8] BOUBLIK, T., 1987, *J. Chem. Phys.*, **87,** 1751.
[9] VEGA, C., and FRENKEL, D., 1989, *Molec. Phys.*, **67,** 633.
[10] SEVILLA, P., and LAGO, S., 1985, *Comput. Chem.*, **9,** 39.
[11] LAGO, S., and SEVILLA, P., 1988, *J. Chem. Phys.*, **89,** 4349.
[12] SEVILLA, P., LAGO, S., VEGA, C., and PADILLA, P., 1991, *Phys. Chem. Liq.*, **23,** 1.
[13] BOUBLIK, T., and NEZBEDA, I., 1977, *Chem. Phys. Lett.*, **46,** 315.
[14] BAXTER, R. J., 1970, *J. Chem. Phys.*, **52,** 4559.
[15] CONROY, H., 1967, *J. Chem. Phys.*, **47,** 5307.
[16] LAGO, S., and VEGA, C., 1988, *Comput. Chem.*, **12,** 343.
[17] JACOBSEN, R. T., and STEWART, R. B., 1973, *J. Phys. Chem. Ref. Data.*, **2,** 757.
[18] BOUBLIK, T., 1981, *Molec. Phys.*, **42,** 209.
[19] VEGA, C., and LAGO, S., 1991 *Molec. Phys.*, **72,** 215.